Z-pinch instability with distributed current

N. R. Pereira, N. Rostoker, and J. S. Pearlman
Maxwell Laboratories, Inc., San Diego, California 92123

(Received 22 July 1983; accepted for publication 14 October 1983)

Sausage and kink growth rates for a Z pinch are computed from ideal magnetohydrodynamic theory for an infinitely thin surface current sheath and for a surface current layer of finite width. The growth rate decreases with increasing layer width. Satisfactory agreement with experiment is obtained for reasonable width estimates based on magnetic field diffusion.

PACS numbers: 52.55.Ez, 52.30. + r, 52.35.Py

I. INTRODUCTION

In Z-pinch experiments at Maxwell Laboratories,[1] growth rates of various instability modes have been measured by observing the variations in optical emission along the pinch axis. For each time, the structure of the optical emission was Fourier decomposed and estimates of the instability growth rates were characterized by wave number k and aximuthal mode number m. Typical growth times[1] are shown in Table I. These growth times were observed for several instability wavelengths; for example, 13 ns was observed for 0.3 and 1.9 cm.

To analyze the instabilities, a model of the pinch was developed in which it was assumed that the implosion and confinement was due to currents on the surface of the plasma column.[2] This assumption appeared valid because of the short times of the plasma dynamics. The predicted growth rates, however, differed from the experimental results by a factor of three.

A simple explanation for this discrepancy could be that the plasma current is carried in a surface layer of finite width. The stability for a pinch with finite width current layer would be intermediate between a sharp boundary pinch (surface current) and a pinch with homogeneous current density, which is marginally stable. In what follows, we will investigate the sensitivity of growth rates to current distribution and use the observed growth rates to estimate the current penetration in the experiments cited above. The results show that the current penetrates through more than half the pinch radius on the time scales of interest.

This estimate compares favorably with the current penetration anticipated from resistive diffusion. The characteristic diffusion time for magnetic field or current is

$$\tau_D = 4\pi r_0^2 \sigma / c^2, \tag{1a}$$

where r_0 is the pinch radius and σ is the conductivity:

$$\sigma \cong 2.5 \times 10^{17}\ \mathrm{T}^{3/2}\ \mathrm{s}^{-1}, \tag{1b}$$

and the temperature T is in kilo-electron-volts.

For the Z-pinch experiment, $T = 0.1$ keV and $r_0 = 1$ mm, hence, $\tau_D = 1\,\mu$s. The time to diffuse a fraction f of the pinch radius is $\tau_D f^2$. Assuming that the available time for magnetic diffusion is equal to the implosion time (80 ns) suggests that the current penetration is about 30%. An alternate estimate assumes that during the collapse, the plasma temperature is probably 20–50 eV, leading to full penetration of the initial, lower, current. In any case, it seems that a finite width current sheath may be present, which would cause the observed growth rates.

Instability growth rates are influenced by more than just the current profile, e.g., initial density and temperature in the pinch, the equation of state, and energy transport. However, these effects seem to be minor for our Z pinches and we will ignore them for now.

II. Z-PINCH MODEL

We consider a model of the pinch that is infinite in the z direction. The plasma, $0 \leqslant r \leqslant r_0$ is assumed to be perfectly conducting and is described by the magnetohydrodynamic (MHD) equations.[3] For $r_0 \leqslant r \leqslant \infty$ we assume that the density vanishes and it makes no difference if the medium is insulating or perfectly conducting. The plasma is treated as incompressible, but some examples of the effect of compressibility will be shown.

The equilibrium MHD equations are

$$\nabla P = -\frac{1}{8\pi}\nabla \mathbf{B}^2 + \frac{1}{4\pi}\mathbf{B}\cdot\nabla\mathbf{B}. \tag{2a}$$

In the present case, $\mathbf{B} = [0, B_\theta(r), 0]$, so that

$$\frac{\partial P}{\partial r} = -\frac{1}{8\pi}\frac{\partial}{\partial r}B_\theta^2 - \frac{B_\theta^2}{4\pi r}. \tag{2b}$$

The linearized perturbation equations are for an incompressible plasma:

$$\delta\rho + \boldsymbol{\delta\xi}\cdot\nabla\rho = 0 = \nabla\cdot\boldsymbol{\delta\xi}, \tag{3}$$

$$-\rho\omega^2\boldsymbol{\delta\xi} = -\nabla\left[\delta P + \frac{B_\theta \delta B_\theta}{4\pi}\right] + \frac{1}{4\pi}(\boldsymbol{\delta B}\cdot\nabla)\mathbf{B} + \frac{B_\theta}{r}\frac{\partial \boldsymbol{\delta B}}{\partial\theta}, \tag{4}$$

TABLE I. Growth times for two representative Z-pinch implosions as measured, compared to the growth times as predicted from the surface current model, Eq. (2).

	Growth times			
	Measured		Predicted	
Array	$m=0$	$m=1$	$m=0$	$m=1$
Low mass, $I = 3$ MA (BLACKJACK 5)	...	14 ns	...	5.7 ns
High mass, $I = 0.8$ MA (BLACKJACK 3)	13 ns	...	3.7 ns	...

 0021-8979/84/030704-04$02.40

$$\delta \mathbf{B} = \nabla \times (\delta \boldsymbol{\xi} \times \mathbf{B}). \tag{5}$$

Assume that $\delta \xi = \xi(k,m,r) \exp i(kz + m\theta - \omega t)$ and a similar form for all perturbations. Then Eqs. (3), (4), and (5) can be reduced to one equation for ξ_r which is

$$\frac{\partial}{\partial r} F(r) \frac{\partial}{\partial r} r\xi_r + G(r)\xi_r = 0, \tag{6}$$

where

$$F(r) = \frac{[4\pi\rho\omega^2 - m^2 B_\theta^2/r^2]r}{(k^2 r^2 + m^2)}, \tag{6a}$$

$$G(r) = \frac{m^2 B_\theta^2}{r^2} - 4\pi\rho\omega^2 - 2B_\theta \frac{\partial}{\partial r}\left(\frac{B_\theta}{r}\right) - \frac{2m^2 B_\theta^2}{r^2(k^2 r^2 + m^2)} + \frac{\partial}{\partial r}\left[\frac{2m^2 B_\theta^2}{r(k^2 r^2 + m^2)}\right] + \frac{4m^2 k^2 r^2 (B_\theta^2/r^2)^2}{(k^2 r^2 + m^2)(4\pi\rho\omega^2 - m^2 B_\theta^2/r^2)}. \tag{6b}$$

The same equations are obtained from the standard equations for a screw pinch [Ref. 3, Eqs. (6.3.2)–(6.3.7)] by omitting compressibility and the axial magnetic field.

The boundary condition on the radial displacement $\delta\xi_r$, is

$$\delta\xi_r = \begin{cases} ar, & \text{for } m = 0, \\ ar^{m-1}, & \text{for } m \neq 0. \end{cases} \tag{7a}$$

The pinch center $\delta\xi_r(r = 0) \exp i(kz + m\theta - \omega t)$ remains unchanged, except for the kink mode $m = 1$. The perturbed pressure $\delta p^* = \delta P + B_\theta \delta B_\theta / 4\pi$ is

$$\delta p^* = \frac{[4\pi\rho\omega^2 - m^2 B_\theta^2/r^2]}{4\pi(k^2 r^2 + m^2)} r \frac{\partial}{\partial r} r\delta\xi_r + \frac{2m^2 B_\theta^2 (\delta\xi_r/r)}{4\pi(k^2 r^2 + m^2)}, \tag{8}$$

for $m = 0$. By substitution,

$$\delta p^*(r = 0) = 2a\rho\omega^2/k^2, \tag{7b}$$

and similarly for $m \neq 0$. Only for the sausage mode, $m = 0$, do these boundary conditions differ from Ref. 3.

At the outer pinch radius r_0, the boundary condition follows from pressure equilibrium with the vacuum region outside the pinch, taken to be of infinite extent. Then

$$\frac{\delta p^*(r_0 - 0)}{r_0 \delta\xi(r_0 - 0)} = -\frac{m^2 B^2}{4\pi r_0^2} \frac{K_m(kr_0)}{kr_0 K'_m(kr_0)}, \tag{9}$$

where K_m is a modified Bessel function, and the argument $(r_0 - 0)$ means that the functions should be evaluated just inside the boundary. The same boundary condition is obtained if the region outside the pinch is a perfect conductor but has zero density.

An incompressible mode for the plasma gives considerably algebraic simplification and is justified because compressibility has little influence on the growth rate for the sharp boundary pinch with constant density. In this case, the growth rate

$$\sqrt{-\omega^2} = (C_A/r_0)\Gamma \tag{10}$$

is determined by

$$\frac{\Gamma^2}{[x^2 + \alpha^2\Gamma^2]^{1/2}} \frac{I_m([x^2 + \alpha^2\Gamma^2]^{1/2})}{I'_m([x^2 + \alpha^2\Gamma^2]^{1/2})} = \frac{m^2}{x} \frac{K_m(x)}{K'_m(x)} + 1, \tag{11}$$

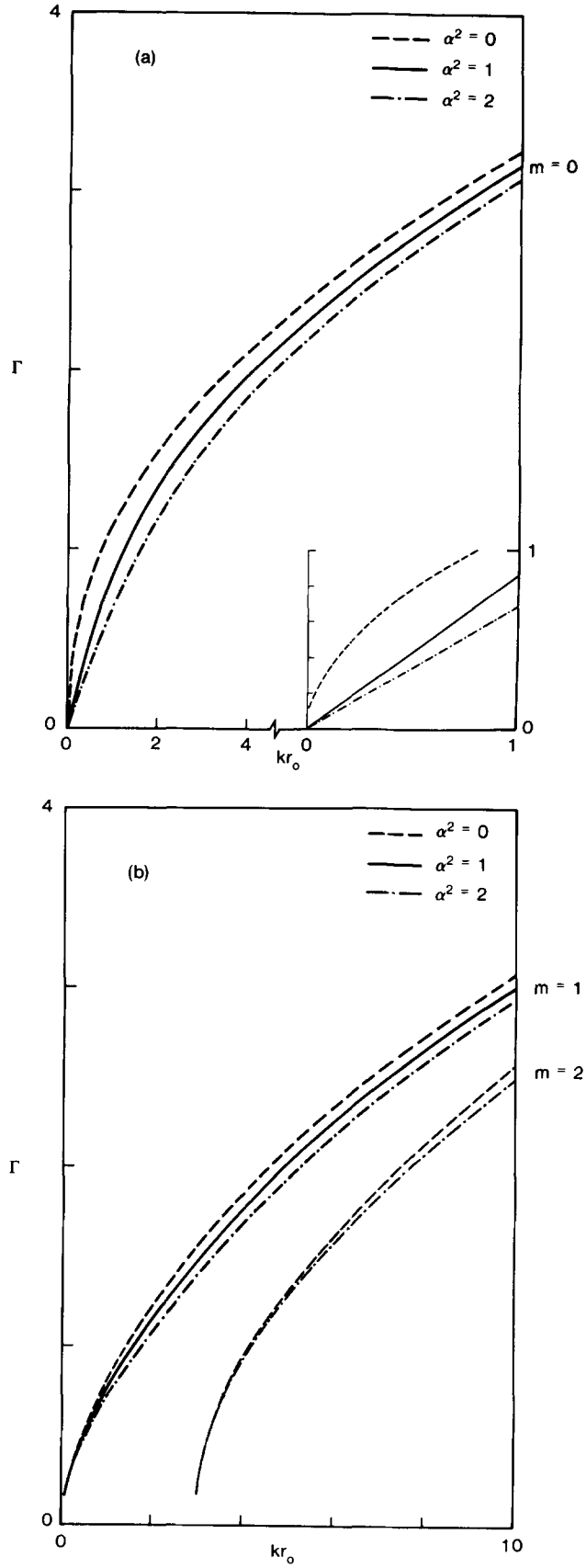

FIG. 1. (a) The growth rate Γ vs wave number $x = kr_0$ for the sausage mode ($m = 0$) in the sharp-boundary pinch, with different compressibilities $\alpha^2 = 0$, 1, and 2. The insert is the region $0 < kr_0 < 1$ on an expanded scale to show the asymptotic behavior near $kr_0 = 0$. (b) The growth rate Γ vs wave number $x = kr_0$ for the kink mode ($m = 1$) and for $m = 2$ in the sharp-boundary pinch, with different compressibilities $\alpha^2 = 0$, 1, and 2.

where C_A is the Alfven speed corresponding to the edge magnetic field B_0;

$$C_A^2 = B_0^2/4\pi\rho, \tag{12}$$

$x = kr_0$, I_m is a modified Bessel function, and the compressibility enters through the ratio of Alfven speed and sound speed C_s,

$$\alpha = C_A/C_s. \tag{13}$$

The sound speed is proportional to the index in the adiabatic gas law $P\rho^{-\gamma} = \text{constant}$,

$$C_S^2 = P/\rho. \tag{14}$$

For an ideal adiabatic gas, $\gamma = 1 + 2/n$, where n is the number of degrees of freedom so that $1 \leqslant \gamma \leqslant 3$. In equilibrium, for which the pressure $P = B_0^2/8\pi$,

$$\alpha = 2/\gamma. \tag{15}$$

The incompressible case corresponds to $\gamma \to \infty$, or $\alpha = 0$, the other limit is the isothermal gas, for which $\gamma = 1$.

For the sausage mode, $m = 0$, Fig. 1(a) shows the growth rate Γ vs kr_0 in (1) the incompressible limit $\alpha = 0$, (2) when $\alpha = 1$, and (3) the isothermal case $\alpha = 2$. The growth rate is insensitive to the value of α, except near $kr_0 = 0$, where the growth rate is

$$\Gamma = (2 - \alpha^2)^{-1/2} kr_0. \tag{16}$$

Figure 1(b) displays the growth rate for the kink mode $m = 1$, and for the next higher mode $m = 2$. Compressibility makes very little difference over the whole range of wave numbers. Therefore, the incompressible model is used in the following analysis. The theoretical values for the growth time in Table I were calculated from Eq. (11) for $\alpha = 0$,

$$\Gamma^2 = \frac{kr_0 I_m(kr_0)}{I'_m(kr_0)} \left[1 + \frac{m^2 K_m(kr_0)}{kr_0 K'_m(kr_0)}\right]; \tag{17}$$

note that this expression should not be used at small kr_0, because for $m = 0$ it gives an erroneous finite limit $\Gamma^2 = 2$ for $kr_0 \to 0$.

Numerical solution of Eq. (6) is necessary to find the growth rate of a Z pinch with finite width current layers. The assumed current distribution is homogeneous in the outer regions of the pinch between $r = Ar_0$ and the edge r_0. The equilibrium pressure in the pinch is no longer constant, but varies with radius according to Eq. (2). The density can be taken constant provided the temperature is consistent. An alternative is to determine the density through either adiabatic compression $p \sim \rho^\gamma$ with $\gamma = 5/3$, isothermal compression where $\gamma = 1$, or better yet, a model where temperature profile is prescribed separately from energy balance considerations that include joule heating. There are no data that

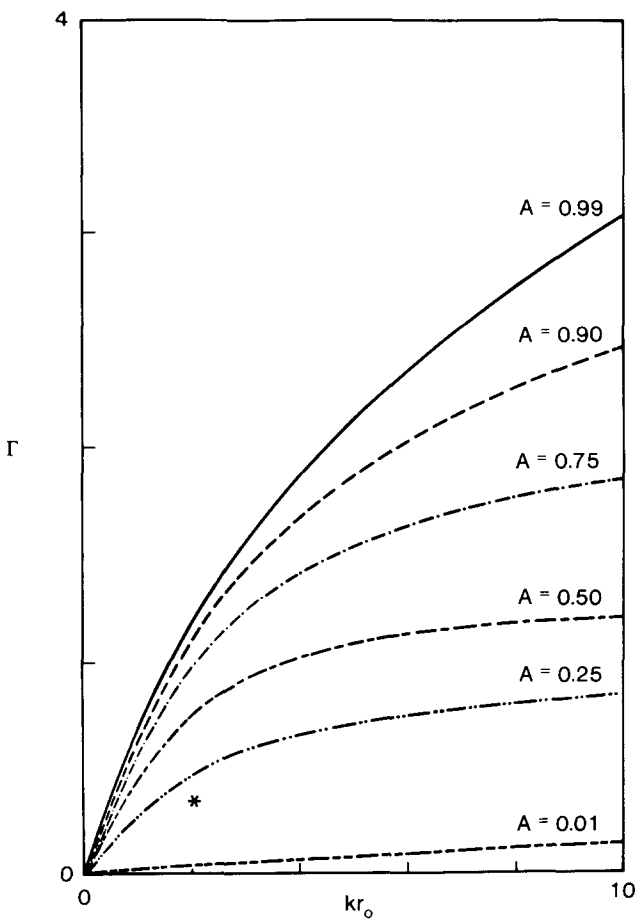

FIG. 2. The growth rate for the sausage mode ($m = 0$) in a constant density pinch with constant current density in a layer between A and 1. The star indicates the experimental value for $\lambda = 0.3$ cm.

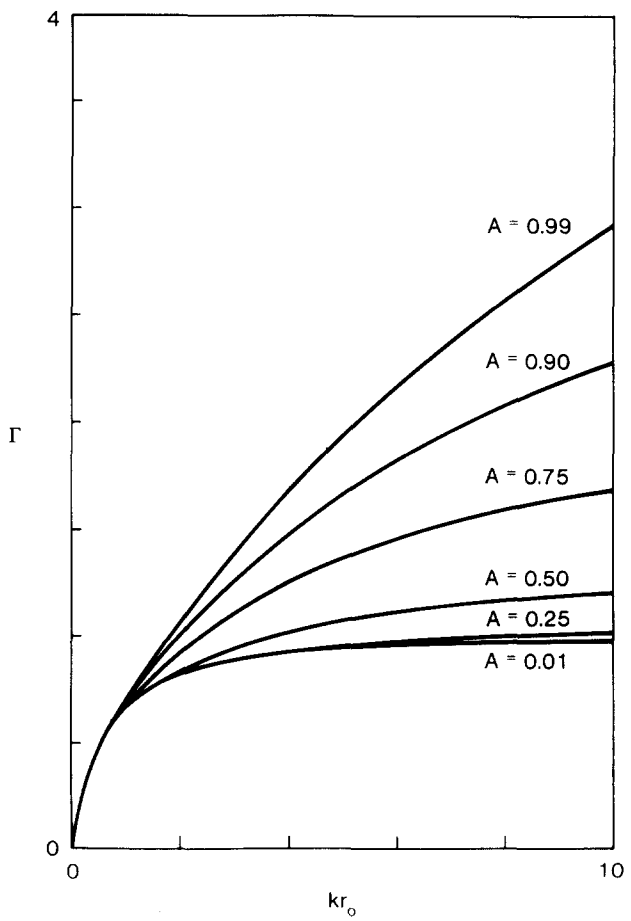

FIG. 3. The growth rate for the kink mode ($m = 1$) in a constant density pinch with constant current density in a layer between A and 1. The growth rate remains finite for equality distributed current ($A \to 0$).

force a particular choice. However, as shown by the growth rates in Figs. 2 and 4, the choice is not particularly important as the density profile makes little difference.

Figure 2 shows the growth rate Γ for the sausage mode ($m = 0$) with a constant density profile and given total current, distributed as a constant current density in a layer from $s = A$ to the edge $s = 1$. At small wavelength $kr_0 \ll 1$ the growth rate is proportional to kr_0, but for $kr_0 \gg 1$ the growth rate saturates. This is particularly pronounced for $A \to 0$, i.e., when the current is evenly distributed. However, where $A \to 0$, the growth rate is relatively small. It is clear that current profile has an appreciable effect on the growth rate; the factor three reduction that is needed for agreement between theory and experiment is obtained for $A = 0.25$ (around $kr_0 \simeq 4$).

Growth rates for the kink mode ($m = 1$) are comparable to sausage instability growth rates. Figure 3 shows the kink growth rates for the current layer model with different layer widths. The growth rates are again proportional to kr_0, and saturate for $kr_0 \to \infty$. For increasingly wide current layers, the growth rates do not decrease to zero but approach a finite value which is roughly a factor three below the growth rate for sharp-boundary pinch. It is, of course, well known that for a Z pinch the kink mode is unstable irrespective of the current distribution, while the sausage mode is stable for the current concentrated near the center.

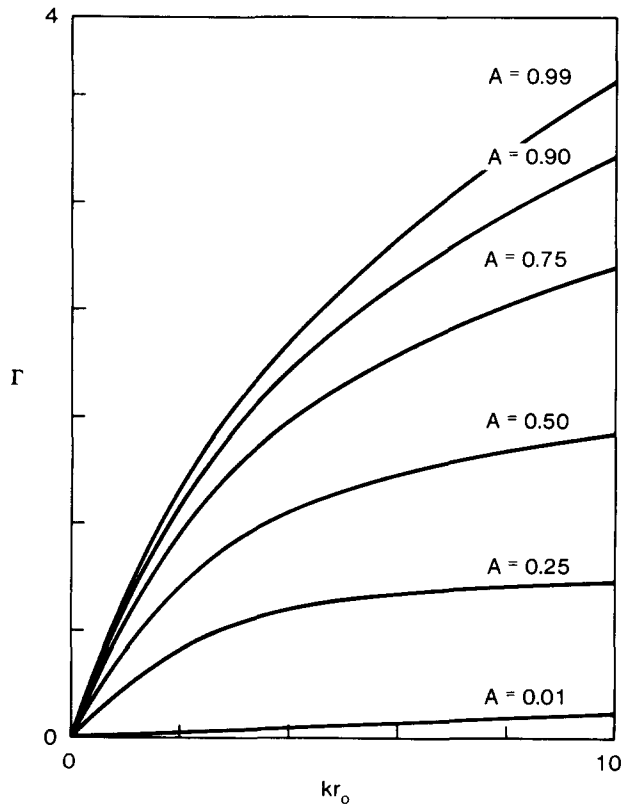

FIG. 4. The growth rates of the sausage mode ($m = 0$) with equilibrium density from adiabatic compression for current density layers of variable width.

Figure 4 shows the sausage mode growth rate Γ assuming adiabatic compression with $\gamma = 5/3$ to determine the equilibrium density. The general behavior of growth rate with wave number is the same as with constant density, but numerically the growth rate is slightly higher when the density is allowed to vary. Note that the relation between the normalized growth rate Γ and the physical value, Eq. (10), is now with the Alfven speed $C_A^2 = B_0^2/4\pi\bar{\rho}$ corresponding to the edge magnetic field and the average density, $\bar{\rho}$, with

$$\bar{\rho}\pi r_0^2 = 2\pi \int_0^{r_0} \rho r dr. \tag{18}$$

The current layer width that gives agreement with experimental growth rates is of the same order but slightly larger than $A = 0.25$ found for a constant density pinch. Apparently these density and temperature profiles have a minor and negligible influence on the growth rates.

III. CONCLUSION

We have investigated sausage and kink growth rates for a Z pinch in which the current is carried in a sheath of finite width. As the sheath thickens, the growth rate decreases. The experimental growth rate is reproduced when the current is homogeneously distributed over the outer 75% of the pinch. Estimates on magnetic field diffusion give similar layer widths.

Other refinements in the MHD model will undoubtedly influence the optimum current width further, but for the moment it suffices that we find a sizable reduction of theoretical growth rates with increasing current layer width. Since the estimated widths are compatible with magnetic diffusion the model gives a consistent interpretation of the experimental data.

ACKNOWLEDGMENTS

We thank J. C. Riordan for his experimental data and discussions, and C. Fowler for help with the computations. This work was sponsored by the Defense Nuclear Agency under contract number DNA001-79-C-0024.

[1]J. S. Pearlman, J. C. Riordan, and N. Rostoker, Maxwell Laboratories, Inc., presented at the APS Plasma Physics Conference, New York, NY (1981), paper 4G9 (to be published).

[2]E. G. Schmidt, *The Physics of High-Temperature Plasmas* (Academic, New York, 1966).

[3]G. Bateman, *MHD Instabilities* (MIT Press, Cambridge, 1978).

[4]J. P. Freidberg, Rev. Mod. Phys. **54**, 801 (1982).